For comparison, the variation of R_G with chain length is also plotted in Figure 7 (dotted curve). Except for $\chi_s = 1$ and $\chi = 0.5$, t_{rms} appears to be larger than R_G. This is in contrast to physically adsorbing chains from solution, in which case t_{rms} is usually smaller than R_G.[16] For $\chi_s = 0$ and $\chi = 0$, t_{rms} is approximately $2.5R_G$. This emphasizes that terminally attached chains can form highly extended layers in comparison with purely physically adsorbed chains from solution.

Conclusion

Both MC and SCF calculations of terminally attached chains predict similar adsorption profiles. Small differences have been accounted for in terms of excluded volume effects and the periodic boundary condition. At high grafted amounts and for low χ_s, highly extended adsorbed layers are formed, emphasizing the usefulness of these systems as steric stabilizers.

References and Notes

(1) Cosgrove, T.; Cohen Stuart, M.; Vincent, B. *Adv. Colloid Interface Sci.* **1985**, *24*, 81.
(2) Crowley, T. L. Ph.D. Thesis, Oxford, 1984.
(3) Cosgrove, T.; Crowley, T. L.; Vincent, B. In *Adsorption from Solution*; Rochester, C. H., Ottewill, R. H., Eds.; Academic: New York, 1983; p 283.
(4) Cosgrove, T.; Heath, T. G.; Ryan, K.; van Lent, B. *Polymer* **1987**, *28*, 64.
(5) Hesselink, F. Th. *J. Chem. Phys.* **1964**, *73*, 3488.
(6) Cosgrove, T. *Macromolecules* **1982**, *15*, 1290.
(7) Croxton, C. *J. Phys. A* **1983**, *16*, 4343.
(8) Dolan, A. K.; Edwards, S. F. *Proc. R. Soc. London, Ser. A* **1975**, *A343*, 427.
(9) Levine, S.; Thomlinson, M. M.; Robinson, K. *Faraday Discuss.* **1978**, *65*, 202.
(10) de Gennes, P. G. *Macromolecules* **1980**, *13*, 1069.
(11) DiMarzio, E. A.; Rubin, R. J. *J. Chem. Phys.* **1971**, *55*, 4318.
(12) Clark, A. T.; Lal, M. *J. Chem. Soc., Faraday Trans. 2* **1975**, *74*, 1857.
(13) Rosenbluth, M. N.; Rosenbluth, A. W. *J. Chem. Phys.* **1955**, *23*, 356.
(14) Silberberg, A. *J. Chem. Phys.* **1968**, *48*, 2835.
(15) Scheutjens, J. M. H. M.; Fleer, G. J. *J. Phys. Chem.* **1979**, *83*, 1619.
(16) Scheutjens, J. M. H. M.; Fleer, G. J. *J. Phys. Chem.* **1980**, *84*, 178.
(17) Yamakawa, H. In *Modern Theory of Polymer Solutions*; Harper and Row: New York, 1971; p 124.

Osmotic Compressibility and Mechanical Moduli of Swollen Polymeric Networks

Ivet Bahar and Burak Erman*

School of Engineering, Boğaziçi University, 80815 Bebek, Istanbul, Turkey. Received November 12, 1986

ABSTRACT: The thermodynamics of polymeric networks subject to the action of a solvent is reviewed. Expressions for the osmotic compressibility and elastic moduli (bulk and shear) of the swollen network are derived in relation to the molecular characteristics of the system. The dependence of the osmotic compressibility on the equilibrium degree of swelling and the solvent quality is investigated. A strong dependence of osmotic compressibility on the nature of the solvent is emphasized. Predictions of the theory are compared with scaling arguments and results of experiments on swollen PVAc networks.

I. Introduction

Early studies of the degree of swelling of networks exposed to a solvent were made on butyl[1] and natural rubbers[2] under uniaxial tension and on natural rubber[3,4] in uniaxial tension, compression, and equibiaxial extension. The relationship of the volume changes to elongation in poly(dimethylsiloxane) networks in uniaxial extension[5] was analyzed at different solvent activities. More recently, the mechanical behavior of swollen polymer networks was analyzed by experiments such as dynamic (quasi-elastic) light scattering, osmotic deswelling, and uniaxial compression.[6,7]

Interpretation of results of the experiments outlined above may suitably be made by thermodynamic arguments that rest on the proper representation of the total free energy of the network–solvent system. In the present study, the thermodynamics of network–solvent systems are reviewed, with particular emphasis on the formulation of the osmotic compressibility and elastic modulus in terms of solution properties and network constitution.

In section II, the general thermodynamic formulation is presented. The total free energy is assumed to be the sum of the free energy of mixing and the elastic free energy of the network. The solvent chemical potential, the os-

motic compressibility, and the elastic moduli (bulk and shear) of the swollen network are derived.

In section III, the dependence of the osmotic compressibility on the equilibrium degree of swelling and on the χ-parameter is explored. In many real systems, departures from a regular solution are attributed to the concentration dependence of the polymer–solvent interaction parameter which plays a major role in critical transitions. It is shown that for a unique value of the concentration-dependent χ-parameter critical conditions may indeed result, leading to infinite osmotic compressibility. In section IV, the theoretically predicted osmotic compressibility and the elastic modulus of a swollen network are compared with experimental data. The present theory, which basically parallels the treatment of ref 1–5, is compared in the last section with recent scaling arguments.

II. General Formulation

Deformation of Swollen Networks. The state of deformation in a polymeric network under stress may be decomposed into a dilation and a distortion term as[8]

$$\lambda = (v_2^0/v_2)^{1/3}\alpha = (V/V^0)^{1/3}\alpha \tag{1}$$

Here v_2^0 is the volume fraction of the polymer during

cross-linking, and v_2 is the volume fraction in the swollen system under stress. V^0 and V are the corresponding volumes of the sample. λ is the displacement gradient tensor defined by the relation $\lambda_{ij} = \partial x_i/\partial x_j{}'$, where x_i is a coordinate of a point in the network in the deformed state and $x_j{}'$ is a coordinate of the same point in the reference state, i.e., the state of cross-linking. The three principal components of λ are denoted by λ_t, $t = 1, 2, 3$. The tensor α is defined as $\alpha_{ij} = \partial x_i/\partial x_j{}''$, where $x_j{}''$ represents a coordinate of the point in the sample isotropically dilated to the volume V. The tensor α defined in this manner is a measure of distortion at constant volume and by definition its determinant equals unity. The term $(v_2{}^0/v_2)^{1/3}$ or $(V/V^0)^{1/3}$ denotes the isotropic dilation of the network.

For a swollen network under uniaxial stress in the x_1 direction, letting $\lambda_1 = \lambda$, the two lateral components of the extension ratio are obtained from eq 1 as

$$\lambda_2 = \lambda_3 = [v_2{}^0/(v_2\lambda)]^{1/2} \qquad (2)$$

The coefficient of dilation, η, for such a network is defined[5,8] as

$$\eta = (\partial \ln V/\partial \ln \lambda)_{T,p,\mu_1} =$$
$$(\partial \ln V/\partial \ln \lambda)_{T,p,n_1} + (\partial \ln V/\partial n_1)_{T,p,\lambda}(\partial n_1/\partial \ln \lambda)_{T,p,\mu_1} \qquad (3)$$

where n_1 is the number of solvent molecules and the subscript p denotes the pressure which may be identified with the negative of the stress along the transverse directions.[8]

The first term in eq 3, which is designated by η_c, represents the coefficient for the change in volume of the closed system at fixed composition. It may be expressed in terms of the pressure as[5]

$$\eta_c = (\partial \ln V/\partial \ln \lambda)_{T,p,n_1} = \lambda\kappa_L(\partial p/\partial \lambda)_{T,V,n_1} \qquad (4)$$

where

$$\kappa_L = V^{-1}(\partial V/\partial p)_{T,n_1,\lambda} \qquad (5)$$

is the isothermal compressibility at fixed length.

The second term in eq 3 represents the contribution to dilation from the change in composition. It vanishes for closed systems. In semiopen systems, this term, denoted[5] by η_s, may be derived from the chemical potential μ_1 of the solvent as

$$\eta_s = (\partial \ln V/\partial n_1)_{T,p,\lambda}(\partial n_1/\partial \ln \lambda)_{T,p,\mu_1} =$$
$$(\partial \Delta\mu_1/\partial \ln \lambda)_{T,p,n_1}/v_2(\partial \Delta\mu_1/\partial v_2)_{T,p,\lambda} \qquad (6)$$

The osmotic compressibility κ_{os} is defined by the relationship

$$\kappa_{os} = v_2{}^{-1}(\partial \pi/\partial v_2)_{T,p,\lambda}^{-1} \qquad (7)$$

where π is the osmotic pressure. Substituting eq 7 into eq 6 and replacing π by $-\Delta\mu_1/\bar{V}_1$, where $\bar{V}_1$ is the solvent molar volume, we obtain

$$\eta_s = \lambda\kappa_{os}(\partial \pi/\partial \lambda)_{T,p,n_1} \qquad (8)$$

Equations 7 and 8 are similar in form to eq 5 and 4, respectively, where the isothermal compressibility at fixed length κ_L constitutes the analogue to the osmotic compressibility κ_{os}. The reciprocal of the latter represents the bulk osmotic (compressional) modulus of the network and will be denoted by K_v in the following.[9]

Solvent Chemical Potential and Elastic Moduli. The chemical potential of the solvent in the network at fixed length is given by

$$\Delta\mu_1 = (\partial \Delta A/\partial n_1)_{T,p,\lambda} \qquad (9)$$

where ΔA is the total free energy of the system. When ΔA

is assumed to be the direct sum of the mixing free energy and the elastic free energy, ΔA_{el}, eq 9 may be expressed as

$$\Delta\mu_1 = \ln(1 - v_2) + v_2 + \chi v_2{}^2 + (\partial \Delta A_{el}/\partial n_1)_{T,p,\lambda} \qquad (10)$$

where the solvent–solute interaction parameter χ varies with solute volume fraction as

$$\chi = \chi_1 + \chi_2 v_2 + \chi_3 v_2{}^2 + \dots \qquad (11)$$

The dependence of the parameter χ on composition is well established both theoretically and experimentally.[10,11] The coefficients χ_1, χ_2, ..., are functions of molecular characteristics and temperature, as determined for a number of systems.[10,11] The truncation of the series in eq 12 at the second term is satisfactory for most purposes and will be adopted in the present work.

Recent theoretical and experimental work[12-14] shows that the elastic free energy of a real network may satisfactorily be represented by the following function:

$$\Delta A_{el} = (\xi kT/2)\sum_t(\lambda_t{}^2 - 1) +$$
$$(\mu/2)kT\sum_t[(1 + g_t)B_t - \ln\{(B_t + 1)(g_t + 1)\}] \qquad (12)$$

where

$$B_t = (\lambda_t - 1)(\lambda_t + 1 - \zeta\lambda_t{}^2)(1 + g_t)^{-2} \qquad (13)$$

$$g_t = \lambda_t{}^2\{\kappa^{-1} + \zeta(\lambda_t - 1)\} \qquad (14)$$

Here, ξ denotes the cycle rank, μ denotes the number of junctions of the network, and κ and ζ are two material parameters. κ is a measure of the strength of the constraints operating on the junctions. Depending on the molecular constitution and the cycle rank density of the network, it may assume values from zero to infinity. $\kappa = 0$ and ∞ refer respectively to the phantom and affine network limits. According to theory,[15,16] κ is expressed in terms of molecular characteristics as

$$\kappa = Pv_2{}^0x_c{}^{1/2}/4 \qquad (15)$$

where x_c is the mean number of segments in network chains and the dimensionless parameter P is defined[16] by

$$P = (\langle r^2\rangle_0/x_c)^{3/2}N_A/\bar{V}_1 \qquad (16)$$

Here $\langle r^2\rangle_0$ is the mean-square chain length between cross-links and N_A is the Avogadro number.

The coefficient ζ in eq 13 and 14 represents the nonaffine transformations of fluctuations of junctions from their mean locations.[17] This parameter may be construed to represent the influence of inhomogeneities in the structure and topology of the network.

For uniaxial stress, the elastic contribution to the solvent chemical potential follows from eq 10 and 12 as

$$\Delta\mu_{el}/RT \equiv (\partial(\Delta A_{el}/RT)/\partial n_1)_{T,P,\lambda} =$$
$$(\beta/\lambda)[1 + (\mu/\xi)K(\lambda_2{}^2)] \qquad (17)$$

where

$$K(\lambda^2) = B\{\dot{B}(B + 1)^{-1} + g(\dot{g}B + g\dot{B})(gB + 1)^{-1}\} \qquad (18)$$

with

$$\dot{B} = \partial B/\partial\lambda^2 = (-3\zeta\lambda/2 + \zeta + 1)(1 + g)^{-2} - 2\dot{g}(1 + g)^{-1}B \qquad (19)$$

$$\dot{g} = (\kappa^{-1} - \zeta) + 3\zeta\lambda/2 \qquad (20)$$

and

$$\beta = (\bar{V}_1/RT)(\xi kT/V^0) = (v_2{}^0/x_c)(1 - 2/\phi) \qquad (21)$$

Here ϕ denotes the functionality of the network. Sub-

stitution of eq 17 into eq 10 leads to

$$\Delta\mu_1/RT =$$
$$\ln(1 - v_2) + v_2 + \chi_1 v_2^2 + \chi_2 v_2^3 + \beta\lambda^{-1}[1 + (\mu/\xi)K(\lambda_2^2)]$$
$$(22)$$

for the chemical potential of the solvent in a swollen network under fixed uniaxial strain.

On the other hand, from eq 7, the osmotic compressibility may be written as

$$\kappa_{os} = -(\bar{V}_1/RT)(v_2\partial(\Delta\mu_1/RT)/\partial v_2)^{-1}_{T,p,\lambda} \qquad (23)$$

where $-\Delta\mu_1/\bar{V}_1$ has been substituted for the osmotic pressure π. Using, in eq 23, the expression for the solvent chemical potential given by eq 22, and differentiating with respect to polymer volume fraction cause the bulk osmotic modulus at fixed length to become

$$K_v = \kappa_{os}^{-1} = (RT/\bar{V}_1)[v_2^2(1 - v_2)^{-1} - 2\chi_1 v_2^2 - 3\chi_2 v_2^3 +$$
$$\beta(v_2/v_2^0)\lambda_2^4(\mu/\xi)\dot{K}(\lambda_2^2)] \quad (24)$$

where

$$\dot{K}(\lambda^2) = \partial K/\partial\lambda^2 = B\ddot{B}/(1 + B) + \dot{B}^2/(1 + B)^2 +$$
$$D\ddot{D}/(1 + D) + \dot{D}^2/(1 + D)^2$$

$$\ddot{B} = -[(4\dot{g}\dot{B} + 2\ddot{g}B)/(1 + g) + (2B\dot{g}^2 + 3/4\lambda)/(1 + g)^2]$$

$$\ddot{g} = 3\zeta/4\lambda$$

$$D = Bg$$

$$\dot{D} = \dot{B}g + B\dot{g}$$

$$\ddot{D} = \ddot{B}g + 2\dot{B}\dot{g} + B\ddot{g} \qquad (25)$$

The osmotic compressibility of a network may conveniently be measured in the free undistorted ($\alpha = 1$) state.[7] The linear dilation ratio λ becomes $\lambda = \lambda_1 = \lambda_2 = \lambda_3 = (v_2^0/v_2)^{1/3}$. The expression for $\Delta\mu_1/RT$ in this case is given by eq 22, where λ_2 is replaced by λ. With this expression for $\Delta\mu_1$, the bulk modulus for the unconstrained, undistorted network is obtained as

$$K_v = \kappa_{os}^{-1} = (RT/\bar{V}_1)\{v_2^2(1 - v_2)^{-1} - 2\chi_1 v_2^2 - 3\chi_2 v_2^3 -$$
$$(\beta/3)(v_2^0/v_2)^{-1/3}[1 + (\mu/\xi)K(\lambda^2) -$$
$$2(\mu/\xi)(v_2^0/v_2)^{2/3}\dot{K}(\lambda^2)]\} \quad (24')$$

The tensile force for simple elongation is given by

$$f = L_0^{-1}(\partial\Delta A_{el}/\partial\lambda)_{T,V,n_1} \qquad (26)$$

where L_0 is the length of the isotropic undistorted sample in the direction of stretch, in the reference state of volume V^0, i.e., during cross-linking. The elastic energy is given by eq 12. In this equation the first term represents the elastic free energy of an equivalent phantom network where the junctions and subchains move freely without restraint. The second term accounts for the effect of constraints on the fluctuations of junctions. The latter may be dropped provided that the corresponding constraints are negligibly small, i.e., in situations where the experimentally reported C_2 value of the Mooney–Rivlin equation is equal to zero.[5] In this case, the force in uniaxial deformation becomes

$$f = (\xi kT/L_0)[\lambda - v_2^0/v_2\lambda^2] =$$
$$(\xi kT/L_0)(v_2^0/v_2)^{1/3}(\alpha - \alpha^{-2}) \quad (27)$$

By definition, the shear modulus E_s is expressed in terms of the tensile force f, for an incompressible solid, as

$$E_s = f/3A(\alpha - 1) \qquad (28)$$

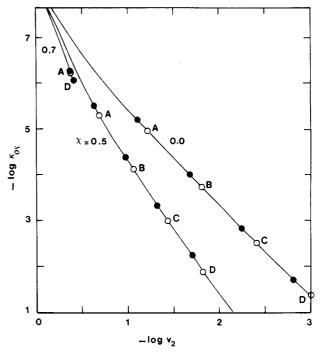where A designates the cross-section of the swollen specimen. Combination of eq 27 and 28 causes the shear

Figure 1. Osmotic compressibility (in N^{-1} m^2) of a perfect tetrafunctional network in terms of the degree of swelling in a solvent with $RT/\bar{V}_1 = 25$ N mm^{-2}. Curves represent results for $\chi = 0.0$, 0.5, and 0.7. The open circles A, B, C, D in each curve are obtained for phantom networks with x_c values of 10^2, 10^3, 10^4, and 10^5, respectively. Calculations for affine networks lead to points situated along the same curves, slightly above those for the phantom network, as shown by the solid circles.

modulus in the limit of small deformations ($\alpha \to 1$) to become

$$E_s = (\xi kT/L_0A)(v_2^0/v_2)^{1/3} = (\xi kT/V^0)(v_2/v_2^0)^{1/3} \quad (29)$$

III. Calculations

Dependence of Osmotic Compressibility on Equilibrium Degree of Swelling. The osmotic compressibility of the network in the undistorted state is given by eq 24', in which the equilibrium degree of swelling is obtained by equating the corresponding chemical potential to zero. Calculations are carried out for a perfect tetrafunctional network, cross-linked in the bulk state; i.e., $v_1^0 = 1$. $RT/\bar{V}_1$ is set equal to 25 N mm^{-2}, and the χ parameter is taken to be independent of concentration ($\chi_2 = 0$). Both affine and phantom limits are considered since real networks are expected to exhibit intermediate behavior. The results of calculations are shown in Figure 1. Logarithmic values are displayed in order to compare the theoretical predictions with scaling arguments (see Discussion). Calculations are made for $\chi = 0.0$, 0.5, and 0.7 to investigate the dependence of κ_{os} on v_2 in athermal, Θ, and poor solvents, respectively.

Each curve in Figure 1 is obtained by varying x_c. The open circles A, B, C, and D on each curve are obtained for phantom networks with x_c values of 10^2, 10^3, 10^4, and 10^5, respectively. An interesting feature that follows from calculations is that virtually the same curves are obtained for both affine and phantom networks. Results of the calculations for $x_c = 10^2$, 10^3, 10^4, and 10^5, for an affine network are shown by the solid circles located slightly above the corresponding phantom network results.

In the athermal and Θ solvents, an increase in chain length results in a strong increase in the osmotic compressibility as seen from the corresponding curves in Figure 1. For a network in an athermal solvent, $\kappa_{os} = 10^{-5}$ and 0.5 N m^{-2} for $x_c = 10^2$ and 10^5, respectively. The depen-
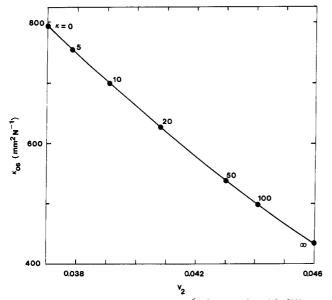
Figure 2. Relationship of κ_{os} to v_2 for real networks with different degrees of constraint, represented by the κ values along the curve. Results of calculations for $\zeta = 0$, $\chi = 0.5$, $x_c = 10^4$, and $v_2{}^0 = 1$ are presented.

dence of κ_{os} on x_c is significantly diminished, however, for networks in poor solvents. For $\chi = 0.7$, $\kappa_{os} = 5 \times 10^{-7}$ N m^{-2} and 8×10^{-7} N m^{-2} for $x_c = 10^2$ and 10^5, respectively. For Θ and good solvents, the osmotic compressibility increases without bound as x_c increases, whereas it converges to a finite value for poor solvents. The terminal point on the curve for $\chi = 0.7$ designated by D in Figure 1 also represents the limit as x_c tends to infinity.

Calculations for real networks lead to points between the phantom and the affine limits. The relationship of κ_{os} to v_2 for real networks with different degrees of constraint is displayed on a nonlogarithmic scale in Figure 2, corresponding to $\zeta = 0$, $\chi = 0.5$, $x_c = 10^4$, and $v_2{}^0 = 1$. The different points on the curve show results for networks identified by the indicated constraint parameter, κ. The value of κ for a given network is determined by eq 15. For PVAc networks in acetone, for example, considered in the present study (see section IV), $P = 1.5$ as follows from eq 16. The corresponding κ for the network with $x_c = 10^4$ is calculated to be 37.5 from eq 15.

The dependence of osmotic compressibility on the χ parameter is further investigated in Figure 3, where κ_{os} values from eq 24$'$ are plotted for a network with $P = 1.5$, $\zeta = 0$, $x_c = 10^5$, and $v_2{}^0 = 1.0$ as a function of χ_1 in the interval $0.4 < \chi_1 < 0.60$. The solid curve is obtained by neglecting the concentration dependence of χ, i.e., taking $\chi_2 = 0$. The rapid decrease in κ_{os} is significant as the solvent becomes progressively poorer. The dashed curve is obtained from eq 24$'$ by choosing a fixed value of 0.381 for χ_2 and varying χ_1. This value of χ_2 is deliberately chosen to satisfy critical conditions[16]

$$\Delta\mu_1 = 0 \qquad \partial\Delta\mu_1/\partial v_2 = 0 \qquad \partial^2\Delta\mu_1/\partial v_2{}^2 = 0 \qquad (30)$$

In fact calculations show that the simultaneous solution of eq 30 for the network in consideration leads to $\chi_1 = 0.497$, $\chi_2 = 0.381$, and $v_2 = 0.058$.

The discontinuity at $\chi_1 = 0.497$ in Figure 3 is a natural consequence of the vanishing of the denominator in eq 23 at critical conditions, which also corresponds to the appearance of infinite fluctuations. The abrupt crossover from a good solvent to a poor solvent is clearly visible in the dashed curve of Figure 3. The portion of the curve in the poor-solvent region is very sensitively dependent on
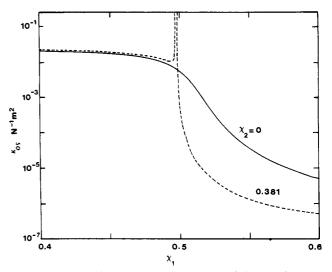

Figure 3. Dependence of osmotic compressibility on the χ parameter near Θ conditions for a swollen network with $x_c = 10^5$, $P = 1.5$, $\zeta = 0$, $v_2{}^0 = 1.0$, and $RT/\bar{V}_1 = 25$ N mm^{-2}. The crossover from good- to poor-solvent regime is accompanied by an abrupt change in κ_{os} as shown by the solid curve. The dashed curve illustrates the behavior of κ_{os} for a system that undergoes critical transition.

χ_2, whereas a negligibly small dependence on χ_2 is observed in the good-solvent region.

An increase in x_c has the same effect as a decrease in $v_2{}^0$ as is apparent from eq 21. Repeating calculations with various x_c values shows that as x_c increases (or $v_2{}^0$ decreases) the portion of the curve in the good-solvent regime in Figure 3 shifts toward higher values while κ_{os} in the poor-solvent regime remains approximately the same. Thus the decrease in κ_{os} during crossover is more pronounced with higher x_c or equivalently lower $v_2{}^0$ values.

IV. Comparison of Calculations with Experiment

Results of osmotic deswelling and compression experiments on poly(vinyl acetate) PVAc networks[7] are shown in Figures 4 and 5. The gels were cross-linked in solution. Osmotic compressibility measurements were performed by deswelling the networks by bringing the swollen system into contact with a solution of known activity through a semipermeable membrane. Acetone and toluene were used as solvents. Results of measurements on the PVAc–acetone system are presented only.

The bulk moduli determined in this manner are shown in Figure 4. Values of the bulk moduli are given along the ordinate in terms of the function $\log (v_2/K_v)$. Open circles represent the result of measurements. The dashed curve is calculated theoretically from eq 24$'$ with the interaction parameter as the previously reported[18] value of $\chi = 0.437$. The solid curve is obtained by assuming a concentration-dependent function as $\chi = 0.437 + 0.2v_2$. The C_2 term of the Mooney–Rivlin equation was reported[7] to be zero for all of the networks, indicating that the contribution of constraints to the moduli was negligible. This may predominantly be due to the fact that the networks were prepared at high dilutions. Consequently κ and ζ were set equal to zero. $RT/\bar{V}_1$ was taken as 35 N mm^{-2}. Each curve represents the locus of points obtained by varying $\xi kT/V^0$ (i.e., β) in eq 24$'$. Calculations for $v_2{}^0 = 0.03$ and 1 resulted in approximately the same curve, indicating that conditions of preparation of the network do not affect the $\log v_2/K_v$ vs. $\log v_2$ curve.

The shear moduli of the swollen networks were independently measured[7] under uniaxial compressive stress. The reported shear moduli of the swollen poly(vinyl ace-
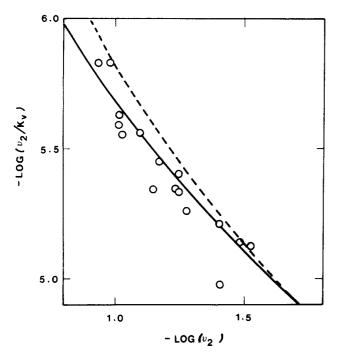
Figure 4. Comparison of experimental and theoretical values of the bulk moduli of PVAc networks swollen in acetone. Points show the results of experiments on samples of different cross-link densities.[7] The dashed curve is obtained from theory with $\chi = 0.437$. The solid curve represents calculations with $\chi = 0.437 + 0.2v_2$.
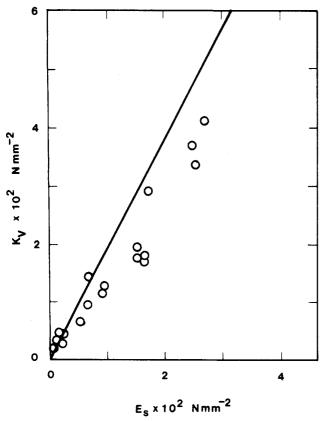

Figure 5. Comparison of the bulk and shear moduli of PVAc networks in acetone. Circles represent experimental results.[7] The straight line is obtained according to the theory from eq 24' and 29.

tate) networks in acetone may be calculated with eq 29. In Figure 5, values of bulk moduli, K_v are shown in terms of the corresponding shear moduli E_s. The points represent results from experiments.[7] The straight line is ob-

tained by employing eq 24' and 29 according to which the ordinate and the abscissa are calculated. Same parameters as those in Figure 4 were used. The experimentally observed proportionality between K_v and E_s is predicted by the theory as shown by the straight line in Figure 5. However, the slope of the theoretical curve is about 30% larger than that obtained by experiments.

V. Discussion

In the present study, the osmotic compressibility and the elastic moduli of the swollen polymer networks are investigated in relation to their molecular constitution and solvent characteristics. The theory allows for the quantitative prediction of κ_{os}, K_v, and E_s over a broad range of solvent quality, encompassing the transition from the good-solvent regime to the poor-solvent one. Satisfactory agreement is obtained between the theoretically predicted elastic moduli and those observed in osmotic deswelling and compression experiments carried out with PVAc networks swollen in acetone, a system representative of the behavior in good solvent.

In recent years, much work has accumulated on interpreting results from mechanical measurements in terms of scaling arguments.[19] A fundamental relationship that plays a major role in scaling considerations is the proportionality

$$R \sim N^\nu \qquad (31)$$

where R and N stand for the counterparts of $\langle r^2 \rangle^{1/2}$ and n of the classical approach. The exponent ν assumes the values $3/5$, $1/2$, and $1/3$ in good, Θ, and poor solvents, respectively. The former two values follow readily from the mean field approach formulated by Flory[20] as pointed out by de Gennes,[19] while the latter results from the spherical volume occupied by a collapsed coil. Power laws between osmotic pressure, elastic moduli, screening length, etc., and polymer concentration rest upon the use of the above fundamental proportionality and thus are quantitatively valid to the extent that the numerical values of ν are correct. In fact, the concentration dependence of the elastic modulus E (shear and/or bulk modulus) is predicted by scaling arguments as

$$E \sim v_2{}^m \qquad (32)$$

where the power-law exponent m is related to ν by

$$m = 3\nu/(3\nu - 1) \qquad (33)$$

Accordingly, m in eq 32 assumes the values 2.25, 3.0, and ∞ in good, Θ, and poor solvents, respectively. Thus the curves $\log E$ vs. $\log v_2$ (or alternately $\log \kappa_{os}$ vs. $-\log v_2$) are expected to be linear, with slope m according to scaling arguments. However careful examination of Figure 1 shows that although the curves obtained by the present analysis are almost linear the attempt to formulate a scaling relationship of the form $\kappa_{os}{}^{-1} = K_v \sim v_2{}^m$, as in eq 32, fails, unless a limited range of degree of swelling is considered. Calculations based on the present molecular treatment show that, in Θ solvent, m assumes the values of 2.94, 3.13, and 3.52 when $v_2 = 0.015$, 0.09, and 0.35, respectively. Additional calculations not reproduced in Figure 1 for clarity yield $m = 1.94$, 2.07, 2.27, and 2.30 for $v_2 = 0.01$, 0.04, 0.10, and 0.16 in a good solvent with $\chi = 0.2$. Thus in both cases the one-to-one correspondence with the powers $m = 3$ and $m = 2.25$ for Θ and good solvents occurs only within specific concentration ranges. In the limit as v_2 goes to unity, calculations show that m approaches infinity irrespective of solvent quality.

The value $m = \infty$ in poor solvents is representative of the rapid collapse accompanying the Θ transition. In fact such an abrupt change in κ_{os} can be clearly seen from

Figure 3. At critical conditions the osmotic compressibility goes to infinity and then suddenly drops to substantially low values as shown by the dashed curve. However, the present theory also predicts an increased sensitivity of κ_{os} on v_2 slightly before critical conditions are attained (the solid curve in Figure 3). These predictions are in qualitative agreement with recent experiments[21] carried out in the vicinity of the Θ temperature with PVAc in isopropyl alcohol. The apparent exponent m is reported to vary between 2.31 and 13.3, though no collapse of the gel systems is observed.[21]

According to eq 32 and 33, the slope of the line log v_2/K_v vs. log v_2 must be equal to -1.25. The experimentally observed[7] values exhibit a slope equal to -1.4. Zrinyi and Horkay argue[7] that this slope is substantially larger than the value of -1 predicted by the mean field formalism but rather approaches the value of -1.25 predicted by scaling laws. The exponent -1 deduced from the mean field formalism is based on the truncation of the series expansion of the logarithmic term in eq 22 after the first term. As was pointed out recently,[16] the representation of the combinatory portion of the chemical potential by the truncated virial series is not acceptable unless a manageable number of terms are kept. The terms with powers of v_2 exceeding 1 cannot be neglected, particularly in the semidilute domain. The present work demonstrates that by proper treatment of the theory, i.e., by retention of the logarithmic term and suitable choice of the concentration dependence of the χ parameter, the experimental results are exactly reproducible. The convergence to the slope -1 occurs only in the limit as $v_2 \rightarrow 0$, as the slight curvature of the theoretically obtained curve in Figure 4 indicates.

References and Notes

(1) Flory, P. J.; Rehner, J. *J. Chem. Phys.* **1944**, *12*, 412.
(2) Gee, G. *Trans. Faraday Soc.* **1946**, *42B*, 33.
(3) Treloar, L. R. G. *The Physics of Rubber Elasticity*, 3rd ed.; Clarendon Press: Oxford, 1958.
(4) Treloar, L. R. G. *Trans. Faraday Soc.* **1950**, *46*, 783.
(5) Flory, P. J.; Tatara, Y. *J. Polym. Sci., Polym. Phys. Ed.* **1975**, *13*, 683.
(6) See, for example: Candau, S. J.; Young, C. Y.; Tanaka, T.; Lemarechal, P.; Bastide, J. *J. Chem. Phys.* **1979**, *70*, 4694. Hecht, A. M.; Geissler, E. *J. Phys. (Les Ulis, Fr.)* **1978**, *39*, 631. Geissler, E.; Hecht, A. M. *J. Phys. (Les Ulis, Fr.)* **1978**, *39*, 955. Geissler, E.; Hecht, A. M. *Macromolecules* **1980**, *13*, 1276; *ibid.*, **1981**, *14*, 185. Bastide, J.; Candau, S.; Leibler, L. *Macromolecules* **1981**, *14*, 719. Belkebir-Mrani, A.; Beinert, G.; Herz, J.; Rempp, P. *Eur. Polym. J.* **1977**, *13*, 277. Horkay, F.; Zrinyi, M. *Macromolecules* **1982**, *15*, 1306 and references cited therein.
(7) Zrinyi, M.; Horkay, F. *J. Polym. Sci., Polym. Phys. Ed.* **1982**, *20*, 815.
(8) Flory, P. J. *Trans. Faraday Soc.* **1961**, *57*, 829.
(9) In the literature the osmotic compressibility is also defined[7] as $\kappa_{os} = -\bar{V}_1/(\partial\Delta\mu_1/\partial v_2)$. The bulk modulus is then related to κ_{os} by the relation $K_v = v_2/\kappa_{os}$.
(10) Flory, P. J. *Discuss. Faraday Soc.* **1970**, *49*, 7 and references cited therein.
(11) Koningsveld, R.; Kleintjens, L. A.; Schoffeleers, H. M. *Pure Appl. Chem.* **1974**, *39*, 1.
(12) Flory, P. J. *J. Chem. Phys.* **1977**, *66*, 5720.
(13) Flory, P. J. *Polym. J. (Tokyo)* **1985**, *17*, 1.
(14) Flory, P. J. *Br. Polym. J.* **1985**, *17*, 96. Erman, B. *Br. Polym. J.* **1985**, *17*, 140.
(15) Erman, B.; Flory, P. J. *Macromolecules* **1983**, *16*, 1607.
(16) Erman, B.; Flory, P. J. *Macromolecules* **1986**, *19*, 2342.
(17) Flory, P. J.; Erman, B. *Macromolecules* **1982**, *15*, 800.
(18) Browning, G. V.; Ferry, J. D. *J. Chem. Phys.* **1949**, *17*, 2805.
(19) de Gennes, P.-G. *Scaling Concepts in Polymer Physics*; Cornell University Press: Ithaca, NY, and London, 1980.
(20) Flory, P. J. *Principles of Polymer Chemistry*; Cornell University Press: Ithaca, NY, 1953.
(21) Zrinyi, M.; Horkay, F. *Macromolecules* **1984**, *17*, 2805.

Two-Dimensional NMR Determination of the Conformation of an Alternating Styrene–Methyl Methacrylate Copolymer

Peter A. Mirau,* Frank A. Bovey, Alan E. Tonelli, and Sharon A. Heffner

AT&T Bell Laboratories, Murray Hill, New Jersey 07974. Received January 9, 1987

ABSTRACT: Two-dimensional nuclear Overhauser effects (2D NOE) have been used to study the solution conformation of a strictly alternating styrene–methyl methacrylate copolymer. The average solution conformation is determined by measuring the strength of the dipolar interaction between the methylene protons on the polymer main chain from the rate of buildup and decay of the cross peaks in the 2D NOE spectrum. These rates are inversely proportional to the sixth power of the internuclear distance and are therefore sensitive to the local conformation. The NMR-determined average conformation for the styrene units in cohetero triads is 58 ± 5% tt, 24 ± 5% tg^-, and 18 ± 5% g^+t with the isomeric states distorted by 11° from perfectly staggered to accommodate the bulky phenyl groups. These values are compared with those calculated from rotational isomeric state models.

Introduction

Predicting the macroscopic properties of polymers requires an understanding of their structural and dynamic properties at a molecular level and has been the focus of intensive research. It is experimentally difficult, however, to study the molecular behavior of polymer chains at a local level, and indirect methods are frequently employed.[1,2] Measurements of end-to-end distances or dipole moments are examples of indirect means by which one may hope to deduce local properties—principally bond rotational states—by comparison with theoretical predictions from rotational isomeric state models.[3]

NMR has been extensively employed to determine the structure and dynamics of polymers both in solution and in the solid state.[4,5] Proton NMR has made major contributions to our understanding of the microstructure of synthetic polymers, but during the past 15 years had been largely eclipsed by carbon-13 NMR because of the much greater range of carbon chemical shifts and the corresponding greater sensitivity to structural detail. Proton